

SEA ICE PROCESSES

AD-A193 980



DTIC  
 ELECTE  
 MAY 09 1988  
 S D  
 22D

**DISTRIBUTION STATEMENT A**  
 Approved for public release  
 Distribution Unlimited

2

**SEA ICE PROCESSES**

**SAIC**

Science Applications International Corporation

1304 Deacon  
College Station, Texas 77840

James K. Lewis  
Maria R. Giuffrida  
Warren W. Denner

SEARCHED  
MAY 09 1988  
Dcs

DISTRIBUTION STATEMENT A  
Approved for public release;  
Distribution Unlimited

Final Report to the Naval Ocean Research and Development Activity  
N00014-87-C-0173  
SAIC-87/1870

January 1988

REPORT DOCUMENTATION PAGE

1a. REPORT SECURITY CLASSIFICATION <b>UNCLASSIFIED</b>	1b. RESTRICTIVE MARKINGS
---	--------------------------

2a. SECURITY CLASSIFICATION AUTHORITY	3. DISTRIBUTION / AVAILABILITY OF REPORT  Approved for public release; distribution is unlimited.
2b. DECLASSIFICATION / DOWNGRADING SCHEDULE	

4. PERFORMING ORGANIZATION REPORT NUMBER(S) SAIC-87/1870	5. MONITORING ORGANIZATION REPORT NUMBER(S)
---	---

6a. NAME OF PERFORMING ORGANIZATION Science Applications Int'l. Corp. Applied Environmental Sciences Division	6b. OFFICE SYMBOL (If applicable)	7a. NAME OF MONITORING ORGANIZATION
---	--------------------------------------	-------------------------------------

6c. ADDRESS (City, State, and ZIP Code) 1304 Deacon College Station, Texas 77840	7b. ADDRESS (City, State, and ZIP Code)
--	---

8a. NAME OF FUNDING / SPONSORING ORGANIZATION NORDA	8b. OFFICE SYMBOL (If applicable) Code 311	9. PROCUREMENT INSTRUMENT IDENTIFICATION NUMBER  N00014-87-C-0173
--	--	---

8c. ADDRESS (City, State, and ZIP Code) NSTL, Mississippi 39529	10. SOURCE OF FUNDING NUMBERS		
	PROGRAM ELEMENT NO. PE63704N	PROJECT NO. R1299	TASK NO.

11. TITLE (Include Security Classification)  
Sea Ice Processes

12. PERSONAL AUTHOR(S)  
Lewis, James Kenneth; Giuffrida, Maria Rose; Denner, Warren W.

13a. TYPE OF REPORT Final Report	13b. TIME COVERED FROM 1/1/87 TO 1/1/88	14. DATE OF REPORT (Year, Month, Day) January 1988	15. PAGE COUNT 18
-------------------------------------	--	---	----------------------

16. SUPPLEMENTARY NOTATION

17. COSATI CODES			18. SUBJECT TERMS (Continue on reverse if necessary and identify by block number)  sea ice processes, ice kinematics, thermodynamics, numerical modeling, forecasting
FIELD	GROUP	SUB-GROUP	

19. ABSTRACT (Continue on reverse if necessary and identify by block number)

This report documents the results of a study of a number of sea ice processes in the Arctic Basin. Seasonal sea ice kinematics were closely scrutinized, and their space and time scales calculated. In addition, factors concerning sea ice thermodynamics were considered. Finally, direct comparisons were made between observed ice velocities and corresponding ice velocities from the Polar Ice Prediction System (PIPS). One of the primary objectives of this work was to provide a wide range of information with which one could validate the mechanics and predictions of the PIPS. Factors that were studied include the grid size and time step of the PIPS, the scale of important forcing variables, the formulation of heat fluxes within the model ice field, and steps to be considered in the attempt to produce the most realistic predictions possible.

20. DISTRIBUTION / AVAILABILITY OF ABSTRACT <input checked="" type="checkbox"/> UNCLASSIFIED/UNLIMITED <input type="checkbox"/> SAME AS RPT. <input type="checkbox"/> DTIC USERS	21. ABSTRACT SECURITY CLASSIFICATION
---	--------------------------------------

22a. NAME OF RESPONSIBLE INDIVIDUAL K. Ferer	22b. TELEPHONE (Include Area Code) (601) 688-4760	22c. OFFICE SYMBOL Code 311
---	--	--------------------------------

## EXECUTIVE SUMMARY

This report documents the results of a study of a number of sea ice processes in the Arctic Basin. Seasonal sea ice kinematics were closely scrutinized, and their space and time scales calculated. In addition, factors concerning sea ice thermodynamics were considered. Finally, direct comparisons were made between observed ice velocities and corresponding ice velocities from the Polar Ice Prediction System (PIPS). One of the primary objectives of this work was to provide a wide range of information with which one could validate the mechanics and predictions of the PIPS. Factors that were studied include the grid size and time step of the PIPS, the scale of important forcing variables, the formulation of heat fluxes within the model ice field, and steps to be considered in the attempt to produce the most realistic predictions possible. As such, a number of points resulted, and the more important of these are summarized here:

- 1) Ice divergence is the most temporally and spatially incoherent of the ice kinematic parameters.
- 2) The short space and time scales of ice pack divergence are not reflected in the other ice kinematic parameters.
- 3) Because of the operational and mechanical importance of ice divergence, it is recommended that a reduction of the PIPS time step to the order of 1 to 2 hours be studied.
- 4) Contour maps produced from the PIPS model output can be expected, on the average, to resolve nearly all the significant spatial variations of the ice kinematic parameters.
- 5) Further investigations into the small space and time scales of ice pack divergence are needed.
- 6) An enhancement of the PIPS vertical resolution of sea ice to at least 7 levels should be closely studied and considered. Error estimates for heat fluxes in a 7 level model should be made for various ice thicknesses of  $>2$  m under assorted heating conditions.
- 7) Thermal inertia is important on the time scales over which the PIPS operates. This term should be included in future enhancements of the PIPS thermodynamic expressions.
- 8) The top layer of an ice model should be constructed using an equation with thermal inertia, be 3 to 5 cm thick, and be used for the ice skin temperature.
- 9) Verification of the PIPS thermodynamics should use the under-ice noise data that will be collected by NAVOCEANO over the next 12-15 months.
- 10) The PIPS has a tendency to over-estimate ice speeds, and this is associated with directions that are to the right of the observed motion.
- 11) Better ice velocity predictions should be addressed by providing better ice thickness estimates through more precise model thermodynamics.
- 12) Errors in predicting ice velocity extremes and their exact times of occurrence are likely a result of the large grid size of the Fleet Numerical Oceanographic Center atmospheric model.
- 13) If greater precision is required in predicting the times of ice velocity extremes, the grid size of the atmospheric model should be halved ( $\sim 150$  km). This would also satisfy the requirements of predicting snow and cloud cover for input to PIPS.

TABLE OF CONTENTS

EXECUTIVE SUMMARY.....i

1. INTRODUCTION.....3

2. SPACE AND TIME SCALES.....4

3. THERMAL PROCESSES.....6

4. COMPARISONS BETWEEN MODEL AND OBSERVED ICE VELOCITIES.....10

    November 1987.....10

    January 1988.....10

    Some Comments.....16

ACKNOWLEDGMENTS.....18

REFERENCES.....18

Accession For	
NTIS CRAM	✓
DTIC TAB	✓
Unannounced	✓
Justification	
By _____	
Distribution _____	
Availability _____	
DTIC	_____
A-1	_____



## 1. INTRODUCTION

A number of methods have been developed to monitor various sea ice processes in the arctic. A great deal of observational information is now being supplied by buoys drifting on the ice. Data streams include position, atmospheric pressure, air temperature, under-ice noise, ice temperature variations, and ocean current and temperature structure. This form of remote sensing is one of the most economical methods for data collection and real-time monitoring in the arctic. Unfortunately, ice drifts. As a result, one must seed a region of importance on a regular basis. Also, it is not feasible to seed specific regions of the Arctic Basin and adjacent seas that are in the vicinity of particular countries. Airplane overflights and under-ice operations are additional methods for providing information on sea ice characteristics. But the types of information that can be collected are somewhat limited and, again, there exists constraints as to areas of operations.

To address the above limitations, one may monitor ice characteristics throughout the arctic using numerical simulations. Hibler (1979) and Hibler and Tucker (1979) developed a dynamic/thermodynamic sea ice model which produces results which are in good agreement with general ice conditions. The model, now referred to as the Polar Ice Prediction System (PIPS), has been upgraded and implemented on Navy computers (Preller, 1985), and initial tests and adjustments have been completed. Average percent errors varied from 15% to 40%. This is an excellent start, but the goals of any numerical simulation and forecast are errors in the range of 10% or less. This is especially critical for an operational model such as the PIPS. If decisions as to strategy and tactics are to be based on PIPS forecasts, we must continue to reduce average errors of the predicted variables.

As part of an effort to verify PIPS, Science Applications International Corporation (SAIC) has undertaken a detailed study of sea ice processes, including kinematics, thermal processes, and direct model/observation comparisons. The goal of the effort was to provide information as to processes and their scales (as ascertained by data from drifters) so as to determine if PIPS is handling such processes appropriately. In the development of such a model, many assumptions and parameterizations must be made. This is particularly true in the Arctic Basin, a region of the

world where little data existed and our understanding of some principles was even more non-existent. However, our data from and knowledge of the arctic has increased substantially since the original development of PIPS. We are now at that point in which we can look at some specific sea ice characteristics and determine if the model is handling them in the most correct manner.

The first task dealt with the space and time scales of sea ice kinematics. These relate directly to the time step and the grid size of the PIPS. In terms of time scales, it has been shown that the higher frequency fluctuations of the ice kinematic parameters (e.g., divergence, deformation, etc.) are one to two orders of magnitude larger than the lower frequency oscillations and long term means (Popelar and Kouba, 1983; Colony and Thorndike, 1984; McPhee, 1978). The question is raised as to what time step must the PIPS be run in order to delineate these fluctuations. There is a very important operational consideration here, primarily concerning sea ice divergence (related to the opening and closing of leads). If the time step is too large, only the average divergence will be calculated, and this may be an order of magnitude smaller than the maximum/minimum divergence.

With respect to space scales, Thorndike (1986) presented speed correlation results determined from drift data throughout the arctic and adjoining seas. However, there still exists questions as to seasonal and regional variations. For an operational model, the grid size should be based on a minimum seasonal/regional space scale, not the average. Moreover, the space scale of differential motion must be taken into consideration. For example, divergence typically has a much smaller space scale than that of the other ice kinematic parameters. This is a result of the special interplay of gravity and buoyancy forces which result from horizontal compression and the conservation of mass.

A second task resulted from research being conducted for the Office of Naval Research (ONR). That work dealt with thermal processes within sea ice, and a number of critical factors were determined which directly affect the operating characteristics of PIPS. These factors include the vertical grid size within the ice, the calculation of the skin temperature, and the effects of snow and cloud cover. The PIPS thermodynamic component contains a parameterized formulation fashioned after Parkinson and Washington (1979) and Manabe et al. (1979). A close

study of the thermodynamics, along with corresponding but independent under-ice noise data, has shown that the thermal heat wave in ice cannot be well determined by the PIPS scheme (Lewis and Denner, 1988). This may explain why the PIPS often under-estimates average ice thicknesses. However, overcoming this problem is relatively straight forward.

The final task of this work was a direct comparison of PIPS motion data with arctic drifter data. Some comparisons had been performed by Tucker and Hibler (1987) in the initial verification of the model output. They found that the PIPS had a bias to over-estimate ice speeds, and this problem was addressed by an adjustment to the wind stress determination. The work presented here is a continuation of such comparisons after the wind stress adjustment. It was initially thought that comparisons of ice velocities and differential motion could be made. Unfortunately, access to clusters of drifters to perform the differential motion calculations was not possible. However, we were able to make a number of comparisons of velocities across the Arctic Basin for November 1987 through January 1988.

## 2. SPACE AND TIME SCALES

Ice kinematics can be described in terms of the 4 basic modes of motion: divergence ( $D$ ), vorticity ( $\zeta$ ), deformation rate ( $T$ ), and ice translation ( $U$ ). In this study, seasonal time histories of these ice kinematic parameters (IKP) were calculated using position data from drifting buoys in the arctic during May, August, and November 1979. The results were used to determine seasonal space and time scales of  $D$ ,  $\zeta$ ,  $T$ , and translation speed variations in the arctic. An e-folding scale was used as a measure of the temporal coherency. Spatial variability was defined in terms of the degree of similarity between the magnitudes of a parameter at two locations.

The details of the seasonal space and time scale analyses are given in Lewis et al. (1988). In general, the divergence was the most temporally and spatially variable of the IKP during spring, summer, and fall. In contrast, the translation speed showed the highest degree of temporal and spatial coherency during all seasons.

The size of the ice parcels considered in this study ( $15.8$  to  $61.5 \times 10^3 \text{ km}^2$ ) is of the same order of magnitude as the grid size used in the

PIPS model ( $16.1 \times 10^3 \text{ km}^2$ ). Therefore, direct comparisons of the kinematic results from this study can be made with the IKP determined by the PIPS. We first begin with a discussion of the time scale results. The time scale calculations indicate that significant variations of some ice kinematics can occur on the order of 2 hours (Table 1). The minimum time scales of divergence and deformation were of the order of the sampling interval of the drifter position data (3 hours). Thus, there is the possibility that the average minimum time scales for these parameters may actually be lower than those calculated in this study.

The implication of the time scales is that the pack ice dynamics has an energetic, short time-frame component. And since divergence is involved (see Table 1), that energetic component is not a negligible factor. Divergence of the ice pack deals with the opening and closing of leads and the production of ice ridges (and thicker ice). Thus, divergence is directly linked to the tensile and compressive strength of sea ice, a very important parameter. If one were to only consider the external forcing of arctic pack ice by the atmosphere, he would expect considerably longer time scales for the ice kinematics. The rotation of the earth introduces an additional consideration, the Coriolis effect. From this, one would expect a time scale of about five hours in the arctic, especially under free-drift conditions. But not all of the kinematic parameters always have such a small minimum time scale as the ice divergence. Obviously, there is some other factor to be considered.

One might immediately suspect that the short-term variability is a result of measurement noise. However, upon closer inspection this is seen to be unlikely. First, the methodology in calculating differential motion is one in which the

	Spring	Summer	Fall
D	2.3 - 26.8	2.6 - 15.2	1.7 - 10.1
$\zeta$	8.0 - 38.5	9.2 - 80.0	20. - 46.1
T	10.2 - 32.8	4.9 - 15.9	2.7 - 24.3
U	14.9 - 80.0	13.0 - 31.5	21.3 - 27.4

Table 1. Range of e-folding times (hours) for each ice kinematic parameter during each season. An e-folding time of 80 hours implies that the temporal autocorrelation never fell below  $e^{-1}$ .

**SAIC**

bias of the position error is estimated and then removed (Kirwan and Chang, 1979). Secondly, in almost all cases only the divergence of a cluster had a short e-folding time while the vorticity and deformation had time scales that were up to 8-12 times longer. Finally, low pass filtering the position data (to remove the influence of position errors) had little effect on the time scale results. Data were low passed filtered using a 10.5 hr half-power point filter that passed 95% of the energy at 12 hr. In general, the speed, vorticity, and deformation time scales of the filtered data were similar to those of the unfiltered data (within 10%). The time scales of the divergence using the filtered position data increased from 2-3 hr to 5-6 hr, still 5-7 times smaller than the scales of the other parameters. These factors indicate that position error is not the cause of the short time scales of ice pack divergence.

Divergence over the world's oceans always tends to have a shorter time scale than other modes of motion. This is the natural result of horizontal compression being compensated by vertical motion. In the case of ice, upward motion encounters the retarding force of gravity while downward motion must overcome buoyancy forces of the denser sea water. As a result, there is typically a normal mode of divergence on a geophysical scale with an inertial period (Cushman-Roisin et al., 1985). In the arctic, this is approximately 12 to 13 hrs. It is quite possible that the internal stresses of sea ice introduce additional variability, and this would naturally be seen primarily by the ice divergence. Internal ice pack stresses may be one of the weakest areas of our knowledge of the geophysics of pack ice. If this factor is the cause of the short time scales of ice pack divergence, it would seem reasonable to deal with it on the same time scale in our modeling. Aside from the internal stresses, ice divergence/convergence is of great importance for the operational needs of the Navy (surfacing, firing, etc.). These factors would seem to warrant running the PIPS with a shorter time step, of the order of 1 to 2 hours.

As for space scales, the results are summarized in Table 2. The minimum length scales of divergence and vorticity (110 and 280 km, respectively) are of the order of the distance between the ice parcels considered in this study. The actual space scales for divergence and vorticity may, therefore, be somewhat less than those determined in this analysis. The data suggest that the space scale for divergence may be less than

100 km. We again are faced with the question as to what factor results in such short scales for ice pack divergence? Whatever that factor is, it does not seem to have the same affect on the other ice kinematic parameters. In this case, we expect the atmospheric forcing to be the primary determinant for the space scales of pack ice. The variability of the Coriolis effect might shorten the space scale somewhat, but we would expect only some secondary effects. The compressive and tensile forces of the pack ice again seem to be the likely cause of the shorter space scales for ice divergence. These forces are a function of the spatial orientation of the crystals of the pack ice floes as well as the orientation of the forcing on the individual floes. Although the orientation of the compressive or tensile forces can be determined by an ice model, it is not now possible to determine mean crystalline orientation within a grid cell. As a result, the adjustment of the PIPS grid to a smaller size based on the space scale results (<100 km) does not appear to be warranted at this time. Further investigation is needed.

The space scale analysis allows one to have confidence in IKP contour maps produced from PIPS model output. The grid spacing of the PIPS model (127 km) is of the order of the smaller space scales of the IKP. Thus, contour maps produced from the PIPS model output could be expected, on the average, to resolve nearly all the significant spatial variations in the IKP. As for IKP determined only from drifter data, contour maps can be trusted only when the centroids of the drifter clusters are separated by distances not much larger than the IKP space scales. Contouring data with spatial gaps in cluster centroid positions greater than IKP scales could result in overlooking significant variations in the IKP. The space scale results of this study (Table 2) indicate the following guidelines in contouring IKP from drifter cluster data: cluster centroid spacings of 500 to 1000 km for U and T; 400 to

	<u>Spring</u>	<u>Summer</u>	<u>Fall</u>
D	195	110	160
$\zeta$	345	280	295
T	640	520	415
U	660	705	665

Table 2. Length scales (km) for the ice kinematic parameters for each season.

500 km for  $\zeta$ ; and no more than 200 km for  $D$ , preferably less. In addition, the minimum space scale results ( $\sim 100$  km) indicate that the areal extent of drifter clusters should not be much larger than  $10\text{-}20 \times 10^3 \text{ km}^2$ . Otherwise, significant variations in IKP (divergence, in particular) may not be resolved.

In final summary, the results of this work indicate the following:

1) Ice divergence is the most temporally and spatially incoherent of the ice kinematic parameters.

2) Ice translation speed is the most temporally and spatially coherent of the ice kinematic parameters.

3) The short space and time scales of ice pack divergence are not reflected in the other ice kinematic parameters.

4) Because of the operational and mechanical importance of ice divergence, it is recommended that a reduction of the PIPS time step to the order of 1 to 2 hours be studied.

5) The space scale analysis indicates somewhat smaller scales than the PIPS grid size. However, it is felt that going to a smaller PIPS grid size would not result in more accurate ice motion predictions at the present state of the model technology.

6) Contour maps produced from the PIPS model output can be expected, on the average, to resolve nearly all the significant spatial variations of the ice kinematic parameters.

7) Further investigations into the small space and time scales of ice pack divergence are needed.

### 3. THERMAL PROCESSES

We now turn our attention to the important factor of heat flux in sea ice. This must be handled carefully and correctly in order to make accurate predictions of sea ice thickness and spatial extent. As background, we first consider the governing equations. The vertical flux of heat within sea ice may be written as

$$\rho_I c_I (dT/dt) = d(k_I dT/dz)dz \quad (1)$$

where  $\rho_I$  is the ice density ( $917 \text{ kg/m}^3$ ),  $c_I$  is the specific heat of ice (a function of temperature and salinity),  $T$  is the ice temperature,  $t$  is time,  $z$

is positive upwards from the ice surface, and  $k_I$  is the thermal conductivity of ice ( $2.03 \text{ W m}^{-1} \text{ }^\circ\text{C}^{-1}$ ). Assume that we have surface temperature fluctuations, the magnitude of which decays exponentially with the depth of the ice. If  $\rho_I$ ,  $c_I$ , and  $k_I$  were constant within the ice, then the solution to (1) is

$$T = (T_s - T_b) z / H + T_s + T_s' e^{\alpha z} \cos(ft + \alpha z) \quad (2)$$

where  $T_s$  is the mean surface temperature,  $T_b$  is the mean temperature at the ice bottom,  $H$  is the ice thickness,  $T_s'$  is the amplitude of the surface temperature fluctuations,  $f$  is the frequency of the temperature fluctuations, and  $\alpha^{-1}$  is the e-folding depth of the temperature fluctuations with

$$\alpha = (\rho_I c_I f / 2 k_I)^{1/2}.$$

In this case, the thermal signal travels through the ice as a damped sinusoid. For a daily period and typical values of  $\rho_I$ ,  $c_I$ , and  $k_I$ ,  $\alpha^{-1}$  is of the order of 20 cm. As the frequency  $f$  becomes smaller (as with fluctuations associated with atmospheric fronts),  $\alpha^{-1}$  becomes large. With these conditions, our expression shows that the ice temperatures at various depths would fluctuate in near unison, with the vertical gradient of temperature being close to linear.

In research conducted by Lewis and Denner (1988), a numerical model was generated based on the finite difference approximation of equation (1). It was verified using the analytical solution (2) and a daily heating cycle. It was found that the analytical solution could not be reasonably approximated without using a small vertical grid spacing, 15 cm in their case. This was a result of requiring a resolution fine enough to resolve the sinusoidal variations with the above length scale of  $\sim 20$  cm.

Now consider the vertical resolution of sea ice thermodynamics in the PIPS. At this time, the ice is represented by only one layer, regardless of its thickness. For a daily heating cycle (which will occur approximately half the year), such a configuration can be expected to over-estimate heat coming from the ocean and under-estimate heat coming from (or going to) the atmosphere. Very distinctly, the thermal wave propagating into the ice will not be readily resolved much of the time. An enhancement to the model is now being

**SAIC**

considered which will increase the vertical resolution to 7 layers, equally divided over the ice thickness. This should substantially increase PIPS's capability to resolve the thermal wave in sea ice.

However, there is a consideration to be made. For thicker ice (>2 m), will a vertical resolution of one-seventh the thickness lead to errors of <10%? The goal is to have errors that are negligible with respect to the results, but this may not be possible for thick ice and a daily heating cycle. Since we have an analytical solution, one can easily estimate percent errors for a given thickness versus vertical resolution for the enhancement now being considered.

To numerically model heat flux in sea ice, the ice is divided into  $n$  layers and (1) is approximated in finite difference form as

$$\begin{aligned} H_n \rho_I c_I (dT/dt) & \quad (3) \\ & = 2 (k_{I,n+1}(T_{n+1}-T_n)/(H_{n+1}+H_n) - \\ & \quad k_{I,n}(T_n-T_{n-1})/(H_n+H_{n-1})) \end{aligned}$$

where  $n$  is the layer number (increasing upwards),  $T$  represents the average temperature of the  $n^{\text{th}}$  layer,  $k_{I,n}$  is the thermal conductivity at the bottom of the  $n^{\text{th}}$  layer, and  $H_n$  is the thickness of the  $n^{\text{th}}$  layer. In the top layer of ice, there exist heat exchanges at the ice surface that include sensible and evaporative heat fluxes (QSENS and QEVAP), short wave solar radiation (QSLR), longwave radiation from the ice to the atmosphere (QBI), and longwave back radiation from the atmosphere (QBA). Thus, for the top layer  $n = 1$ , (3) becomes

$$\begin{aligned} H_t \rho_I c_I (dT/dt) = & \quad (4) \\ & \text{QSLR} + \text{QSENS} + \text{QEVAP} + \text{QBI} + \\ & + \text{QBA} - 2 k_{I,t} (T_t - T_{t-1}) / \\ & / (H_t + H_{t-1}). \end{aligned}$$

The above expression accounts for the flux of heat from the underlying layer of ice and from the ice surface.

In near equilibrium conditions, the thermal inertia of the ice layer is small, and  $dT/dt$  can be set to zero. This is what is done in the PIPS. However, the PIPS is now running with a 6 hr time step. With a daily heating cycle, the thermal

inertia of the ice is very distinctly non-zero. Moreover, Lewis and Denner (1988) found that the thermal inertia term was at times quite important during non-daily heating/cooling events (e.g., the passage of frontal systems during the fall and winter). Without  $dT/dt$ , the PIPS ice has no memory of its temperature from the previous 6 hrs. Therefore, it is allowed to make dramatic variations depending on the other terms in the heat balance equation. This is obviously an oversight which can be readily resolved.

We now discuss the calculation of a skin temperature of the ice. This is an important factor since the skin temperature determines the radiative heat flux from the ice (QBI) and is considered in the calculation of sensible heat flux (QSENS). If one examines equations (3) and (4), it is quite easy to come up with the expression

$$\begin{aligned} \text{QSLR} + \text{QSENS} + \text{QEVAP} + \text{QBI} + \\ \text{QBA} = 2 k_{I,t} (T_s - T_t) / H_t \quad (5) \end{aligned}$$

where  $T_s$  is a skin temperature of the ice surface. Previous studies have used the above expression and iterative techniques to calculate  $T_s$  given the left-hand-side of (5) and  $T_t$  (e.g., Semtner, 1976). Lewis and Denner (1988) attempted such a process in their modeling, but found the resulting thermal stresses determined from observed forcing could not match the fracturing levels from corresponding under-ice noise. In-depth investigation of the terms in the equations showed that (5) was responsible for the problem. It can be shown that the effect of (5) is to flux the heat coming from the surface directly down into the center of the first layer of the ice. There is no thermal memory ( $dT/dt$ ) for the top half of the top ice layer. Thus, solving (5) for a skin temperature for the ice neglects thermal inertia at the region of the ice where memory can be expected to be the most important (the region of greatest temperature swings).

There is no simple way by which one can calculate an ice skin temperature. An estimate can be made, however, using equation (4) for a very thin layer of sea ice at the surface. This gives only the average temperature over the layer, but its use with a 3 cm surface layer has been found to produce quite good results and has been verified with under-ice noise data (Lewis and Denner, 1988).

Finally, we wish to discuss the influence of snow cover on heat flux in sea ice. Snow is by

**SAIC**

far a much better insulator than ice. As such, variations in surface heat fluxes may not be significantly detected by pack ice which has a snow cover of 30-40 cm. As a result, heat flux may have a large spatial incoherence due to the effect of variations in the snow depth. Moreover, snow can be blown around by the arctic storms. Thus, a region may have a substantial snow cover on one day (less thermal flux) but no snow the next (greater thermal flux).

Examples of snow coverage effects are shown in Figs. 1 and 2. These show under-ice noise level variations at 1000 Hz (a result of thermal microfracturing) under the influence of daily temperature fluctuations. The atmospheric conditions were that of high pressure, low wind speeds, no clouds, and air temperature variations of  $\sim 8^{\circ}\text{C}$ . The noise levels and their times of occurrences indicate the following:  $< 5$  cm of snow in the southern Beaufort Sea,  $\sim 15$  cm of snow in the northern Beaufort Sea, and 30-40 cm of snow in the eastern and western Beaufort Sea.

Distribution of snow is difficult to detect remotely since it typically has the same color and temperature of the ice pack. And it is not the presence of snow but its depth which is important with respect to thermal processes in sea ice. Thus, there is a need to determine snow fall accumulation and then its redistribution by wind. It may be possible to estimate these factors using numerical atmospheric models. Such models can give precipitation estimates (location and amount) as a function of time. In addition, the planetary boundary layer of these models can provide estimates of wind velocities which can be used in particle transport calculations. In essence, this can be accomplished by adding another two terms in the mass balance expression for snow in the bottom layer of the model. One is a source term which represents the lifting of the snow from the earth's surface (overcoming cohesive forces) by the shearing stress of the wind. The second is a sink term which represents the settling of snow by a dominance of gravitational forces.

The time and space scales of higher frequency noise have been used to imply scales of thermal processes in sea ice (Lewis and Denner, 1988). As seen in Table 3, these scales are relatively small. The smallest space scales of under-ice higher frequency noise are  $\sim 150$  km. However, this scale is typically 2 to 3 times smaller than those of atmospheric heat flux variables (wind velocity, air temperature, radiation, etc.). The data all imply that there are two length scales

	<u>Time Scale</u>	<u>Space Scale</u>
Summer	15-30	300
Fall	5-19	170
Winter	3-15	240
Spring	5-11	300

Table 3. Time scales (hr) and space scales (km) of 1000 Hz arctic ambient noise in  $\mu\text{Pa}$  in the Beaufort Sea as a function of season.

related to sea ice heat flux. The first are of the order of 300 km or greater and include air temperature, solar radiation, wind velocity, and ice skin temperature. The second length scale appears to be related to snow cover (and possibly cloud cover). Snow cover is more variable in space, and the resulting scales are smaller as implied by the fall data shown in Table 3 ( $\sim 150$  km). If numerical atmospheric models are used to estimate heat fluxes related to snow cover, the data would indicate a grid size of the order of 150 km.

It should be mentioned that an excellent opportunity to verify the thermodynamics of PIPS will occur over the next 12-15 months. During that time, the Naval Oceanographic Office (NAVOCEANO) will have 12 acoustic buoys deployed in the arctic. The higher frequency noise level variations can be used to estimate heat fluxes within the ice. These can be compared to the fluxes determined by PIPS for different regions, ice thicknesses, and seasons. Any PIPS enhancements should use the noise data to verify model thermodynamics.

In summary, the results of this work indicate the following:

- 1) Vertical resolution of the thermal heat wave can be obtained with a grid spacing of  $\sim 15$  cm.
- 2) The PIPS vertical resolution of sea ice should be enhanced to at least 7 levels, with error estimates for heat fluxes being made for various ice thicknesses of  $> 2$  m under assorted heating conditions.
- 3) Thermal inertia is important on the time scales over which the PIPS operates. This term should be included in the PIPS thermodynamic expressions.
- 4) The skin temperature of the ice must be determined using expressions which consider the thermal inertia of the top layer of the ice.

**SAIC**

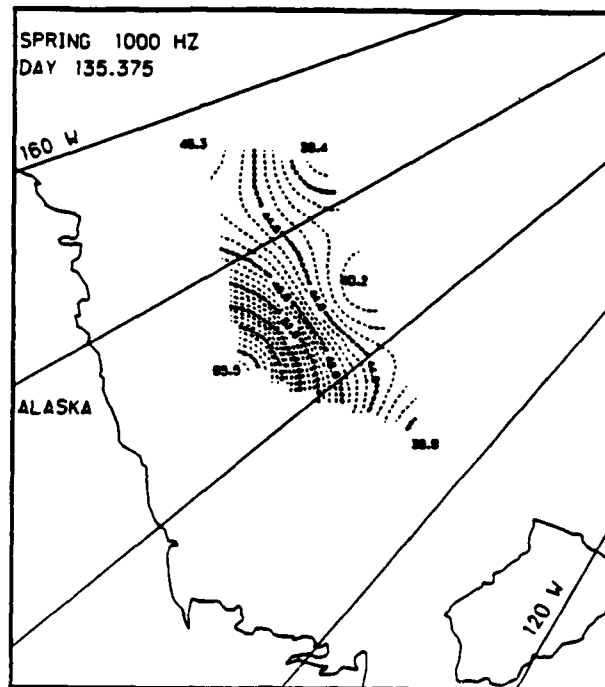


Fig. 1. An example of the effects of snow cover on the spatial variations of 1000 Hz under-ice noise levels at Julian day 135.375 1976. Note the large noise levels in the southern Beaufort Sea, ~25 db higher than at Julian day 135.000.

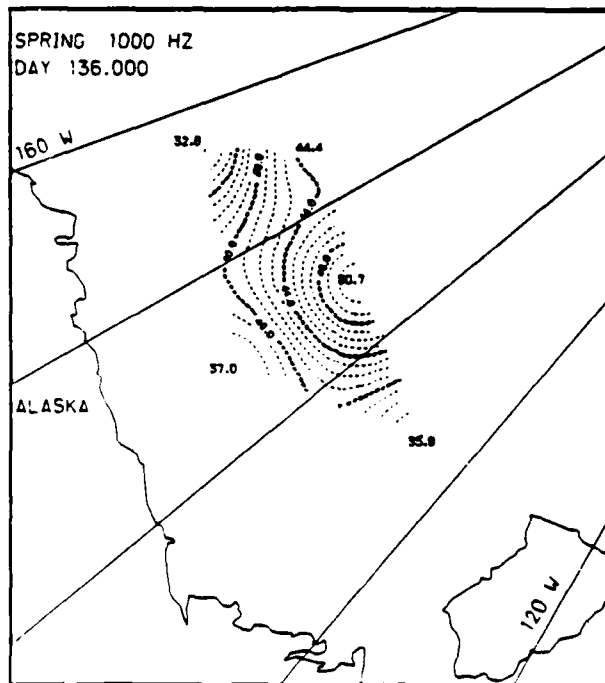


Fig. 2. An example of the effects of snow cover on the spatial variations of 1000 Hz under-ice noise levels at Julian day 136.000 1976. Note that the noise levels in the northern Beaufort Sea have now increased, but only by ~10 db.

5) The top layer of an ice model should be constructed following equation (4), be 3-5 cm thick, and be used for the skin temperature in calculating QSENS and QBI.

6) Snow cover can have a significant effect on sea ice heat fluxes. Snow cover should be estimated using numerical models, but the spatial variability of the snow distribution indicates that such atmospheric models need to operate on a grid size of ~150 km.

7) Verification of the PIPS thermodynamics should use the under-ice noise data that will be collected by NAVOCEANO over the next 12-15 months.

#### 4. COMPARISONS BETWEEN MODEL AND OBSERVED ICE VELOCITIES

A number of comparisons were made of model and observed ice drift. Along with these data, we also considered ice thickness when it was available for the observed drift data. We compared ice speed and direction separately and then together in order to determine if there existed some form of a bias in the model output. Here we will concentrate on three particular regions:

- 1) the Chukchi Sea at about 180°E, 75°N,
- 2) the central polar region (North Pole), and
- 3) the Lincoln Sea north of Greenland, 50°W, 82°N.

Velocity data from these three regions were collected from drifters on the ice. The data were edited for obvious bad data points, fit to one hour intervals, and then averaged over the 6 hr interval that corresponded to output from the PIPS. We will consider two time periods, November 1987 and January 1988.

##### November 1987

The November 1987 raw speed data from the Chukchi Sea is shown in Fig. 3 along with the corresponding PIPS speeds. The PIPS distinctly over-estimates the ice speeds, but in most cases closely follows the speed trends. In Fig. 4 we show the 6 hr average observed ice speeds along with the PIPS data. This plot more clearly demonstrates the PIPS ability to follow many of the oscillations of the observed ice speeds. One notes several instances in which the times of

occurrence of model speed extremes do not precisely match that of the drifter. We will comment on this later.

We compared the model and observed ice speeds in a relative error fashion using

$$(\text{PIPS speed} - \text{observed})/\text{observed}.$$

The results are shown in Fig. 5. Considering the desire to have model errors of the order of 10%, the figures include dashed lines delineating the region of -0.1 to 0.1. Relative errors that fall within that region are defined as acceptable.

The magnitude errors for the Chukchi Sea region show that the model tends to over-estimate ice speeds, with an average error of ~60%. With some adjustment of the time line of the model output, some of these over-estimates could be eliminated. However, the trend would still exist.

Of course, velocity also has a direction, and these differences are shown in Fig. 6. For direction, acceptable errors are defined  $\pm 18^\circ$ . The PIPS was able to provide reliable directional estimates ~50% of the time. For the remainder of the time, the PIPS tended to predict movement to the right of the observed motion. Slight shifts in the time line of the model output would likely reduce some of these directional errors.

There were two drifters in the Lincoln Sea with which we made comparisons for November 1987. The raw speed data are shown in Figs. 7 and 8 along with the PIPS speed data at the particular grid point of the model that covered both drifters. Both raw speed data sets show small mean ice speeds with large oscillations. The PIPS ice speeds correspond more closely with those of buoy 2879. But, in general, there was a distinct tendency for the PIPS to over-estimate these ice speeds.

##### January 1988

The January 1988 raw speed data from the North Pole region are shown in Fig. 9 along with the corresponding PIPS speeds. One notes that the PIPS tends to follow the tops of the peaks in the observed ice speed time histories. In addition, the PIPS did not delineate the observed speed increase that began on Julian day 8. In general, there is a tremendous oscillatory nature in the observed data that cannot be resolved by the PIPS. The differences between the model and observed ice speeds are better pointed out in Fig. 10 which uses the 6 hr average observed speeds. Here it is quite distinct that 1) the PIPS has a bias to over-estimate



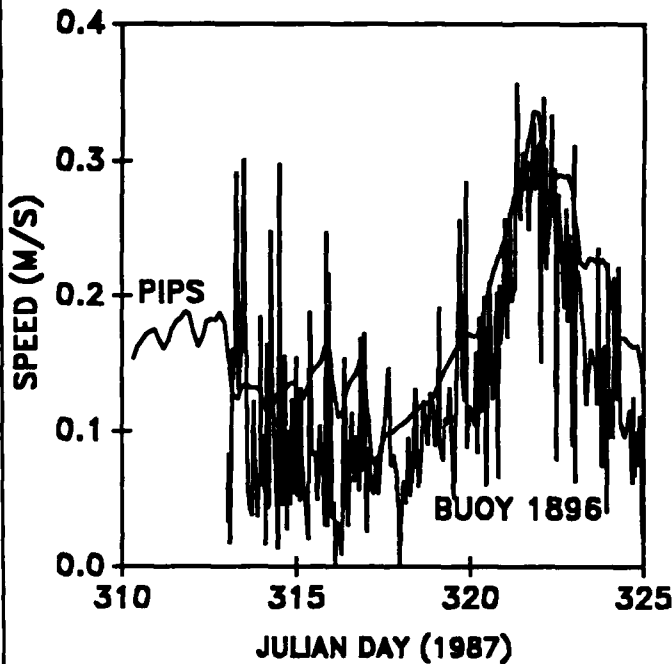


Fig. 3. A comparison of observed ice speeds at Buoy 1896 and PIPS ice speeds in the Chukchi Sea for November 1987.

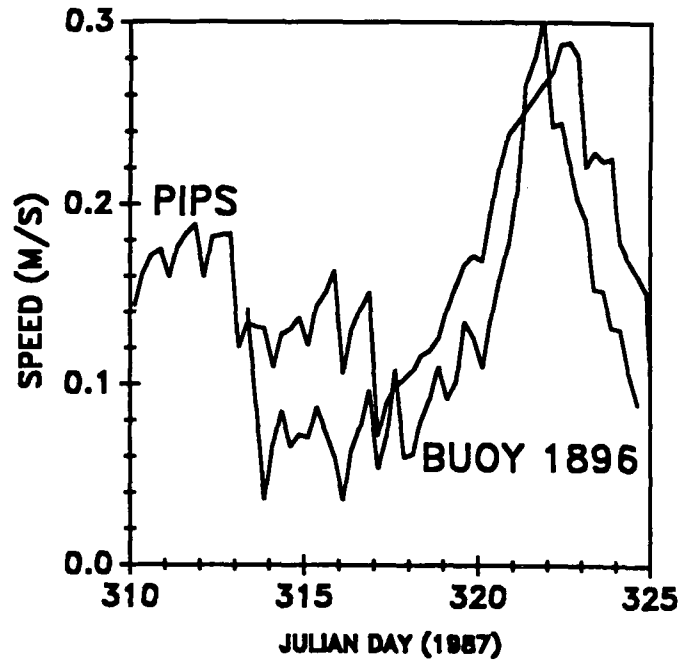


Fig. 4. A comparison of 6 hr averaged ice speeds at Buoy 1896 and PIPS ice speeds in the Chukchi Sea for November 1987.

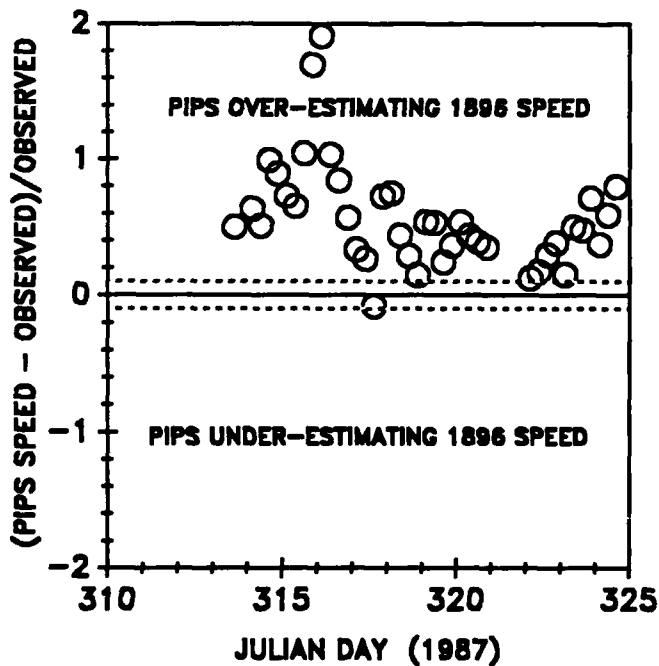


Fig. 5. Relative ice speed errors between the PIPS and 6 hr averaged ice speeds at Buoy 1896 in the Chukchi Sea for November 1987. The dashed lines represent errors of  $\pm 10\%$  which are considered acceptable.

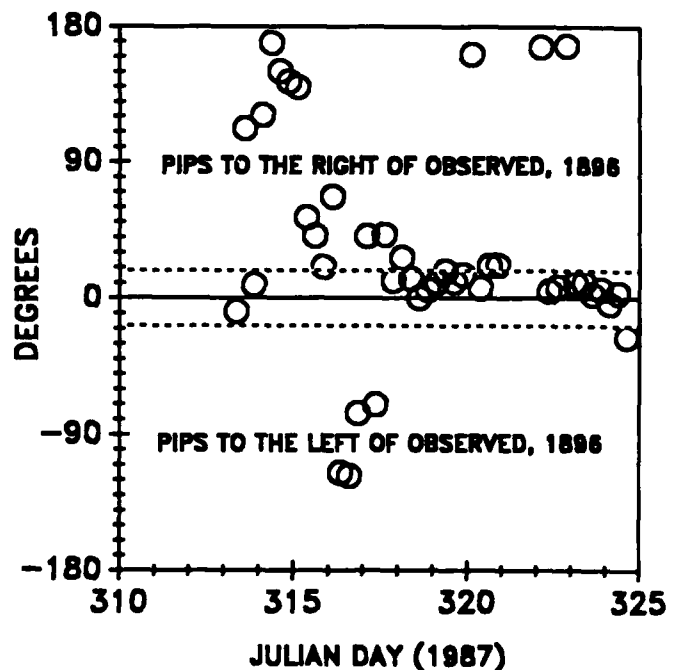


Fig. 6. Directional errors between the PIPS and 6 hr averaged ice motion at Buoy 1896 in the Chukchi Sea for November 1987. The dashed lines represent errors of  $\pm 18^\circ$  which are considered acceptable.

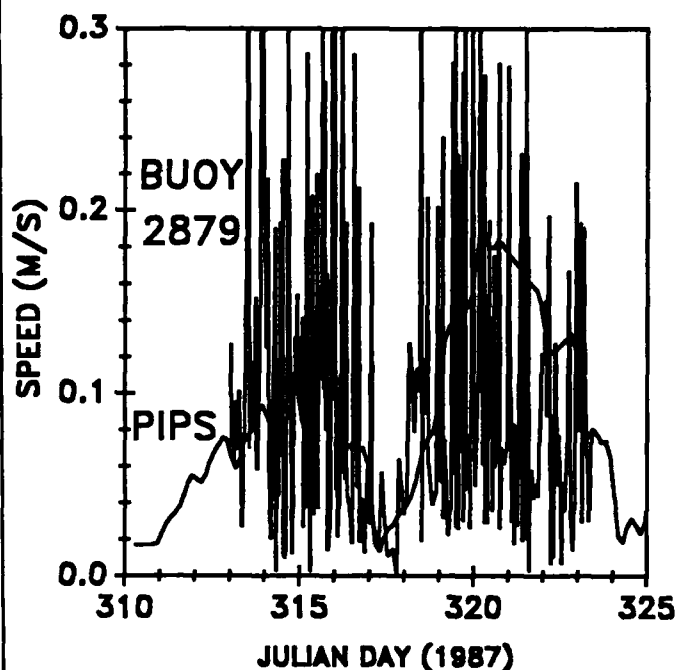


Fig. 7. A comparison of observed ice speeds at Buoy 2879 and PIPS ice speeds in the Lincoln Sea for November 1987.

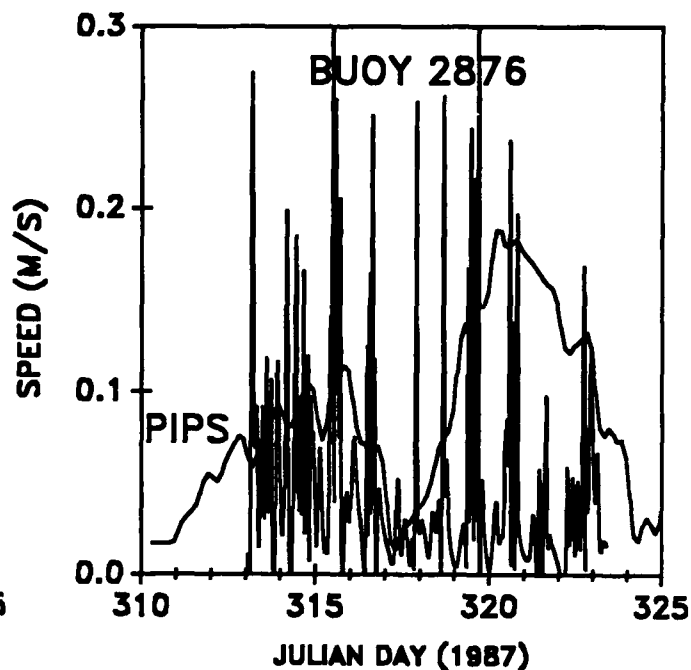


Fig. 8. A comparison of observed ice speeds at Buoy 2876 and PIPS ice speeds in the Lincoln Sea for November 1987.

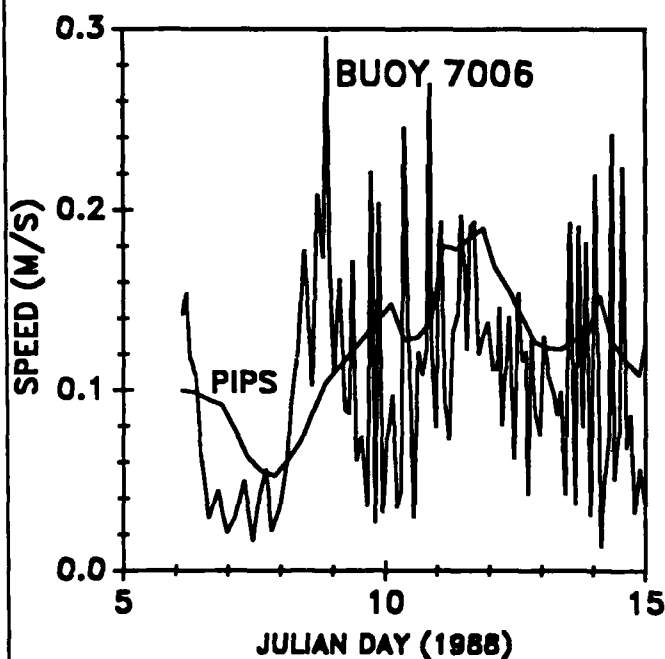


Fig. 9. A comparison of observed ice speeds at Buoy 7006 and PIPS ice speeds at the North Pole for January 1988.

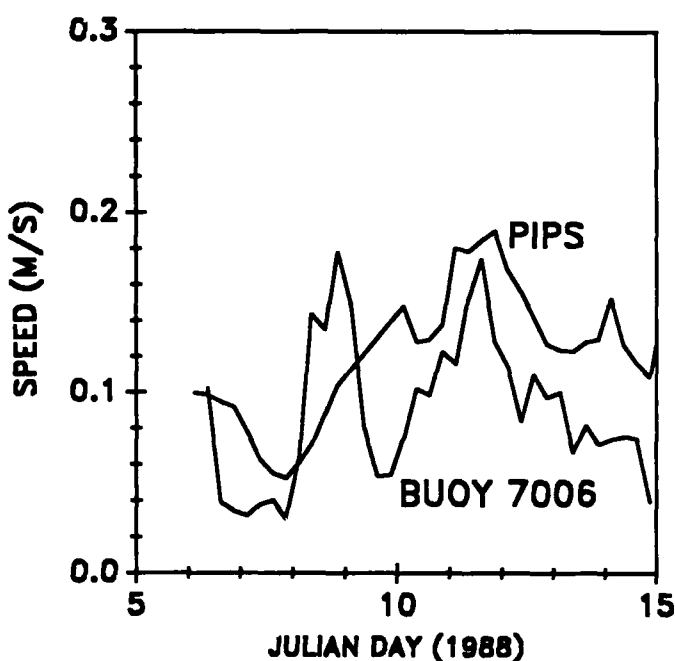


Fig. 10. A comparison of 6 hr averaged ice speeds at Buoy 7006 and PIPS ice speeds at the North Pole for January 1988.

the ice speed and 2) the observed speed has a greater amount of variability.

Another point can be made concerning Fig. 10. This deals with the time differences between the observed and modeled peaks and troughs in ice speed (similar to that of November 1987 for buoy 1896). If one were able to stretch and compress the PIPS speed time history, then we could adjust the model output to match the observed speeds. As it is, there are some time phase errors of the order of  $\pm 1$  day.

As an interesting comparison, we considered the observed and model ice speed data from a location  $\sim 300$  km south of the North Pole. The raw speed and model data are shown in Fig. 11. Again, there are considerable variations in the observed ice speed. The 6 hr average observed and model speeds are shown in Fig. 12. These are quite similar to those seen in Fig. 9, with a slight time difference.

The magnitude errors for the North Pole region (Figs. 13 and 14) show that the model tends to over-estimate ice speeds, with an average error in this case of  $\sim 80\%$ . Once again, some of these over-estimates could be eliminated with an adjustment of the phase of the model time histories.

Directional errors are shown in Fig. 15 for the North Pole. There is a distinct tendency for the PIPS motion to be to the right of the observed motion. In the data from the other station ( $\sim 300$  km south towards Greenland, Fig. 16), the trend for model motion being to the right of the observed motion is not as strong but is still apparent. We point out once again that a phase shift in the model output would eliminate some of this tendency.

During the same time period in January 1988, data were compared from the Chukchi Sea. The raw and model ice speed time histories are shown in Fig. 17. The 6 hr average speeds are shown in Fig. 18, and here we see that the PIPS tends to under-estimate the observed ice speeds. In addition, the minimum in the observed ice speed that occurred at Julian day 10 is totally missed by the model. Under-estimating the ice speed is quantified in Fig. 19 in which the errors are of the order of  $-40\%$ . Directional errors are shown in Fig. 20, with the trend for the model motion to be right of the observed motion still prevalent. As with the previous data, some of these errors could be eliminated with a slight shift in time of the model ice speeds.

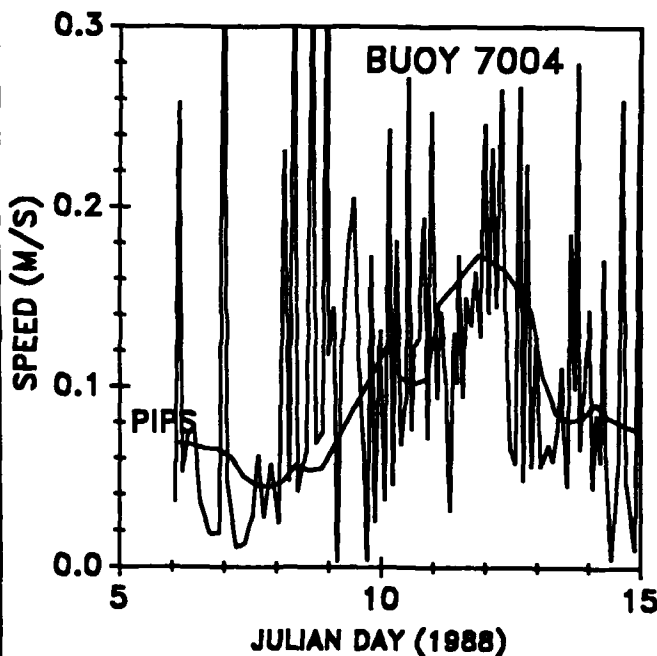


Fig. 11. A comparison of observed ice speeds at Buoy 7004 and PIPS ice speeds just south of the North Pole for January 1988.

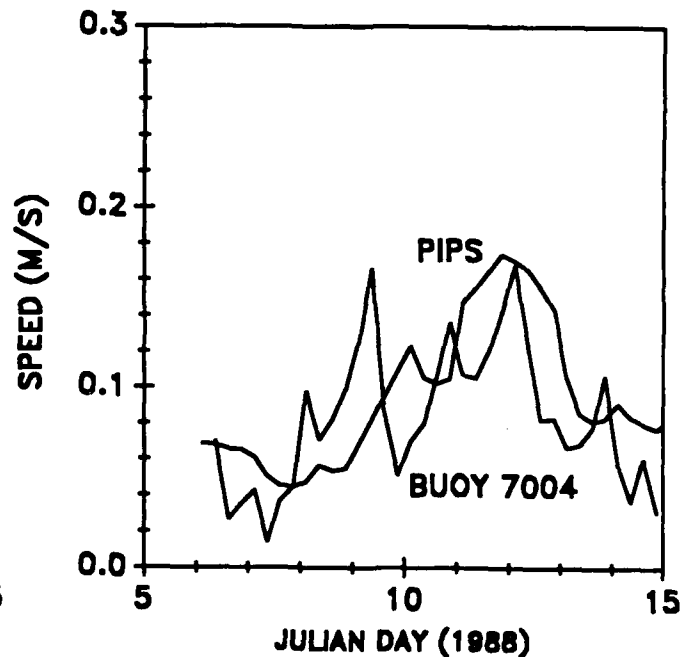


Fig. 12. A comparison of 6 hr averaged ice speeds at Buoy 7004 and PIPS ice speeds just south of the North Pole for January 1988.

**SAIC**

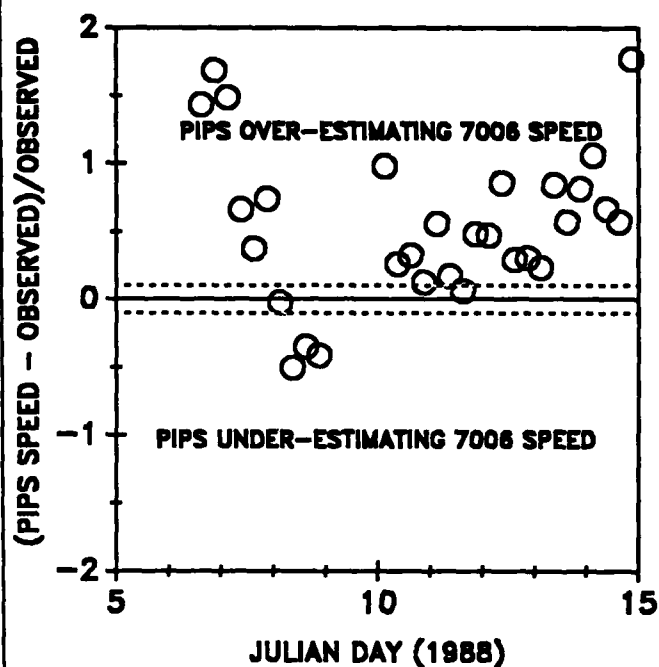


Fig. 13. Relative ice speed errors between the PIPS and 6 hr averaged ice speeds at Buoy 7006 at the North Pole for January 1988. The dashed lines represent errors of  $\pm 10\%$  which are considered acceptable.

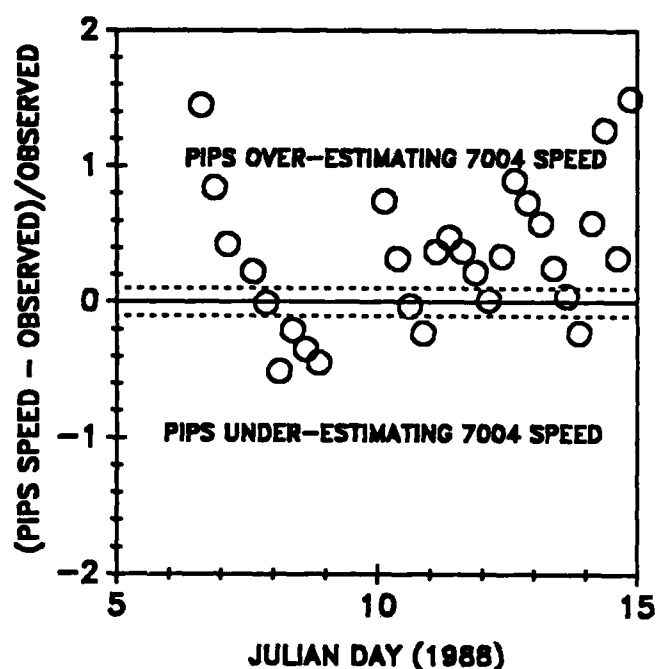


Fig. 14. Relative ice speed errors between the PIPS and 6 hr averaged ice speeds at Buoy 7004 just south of the North Pole for January 1988. The dashed lines represent errors of  $\pm 10\%$  which are considered acceptable.

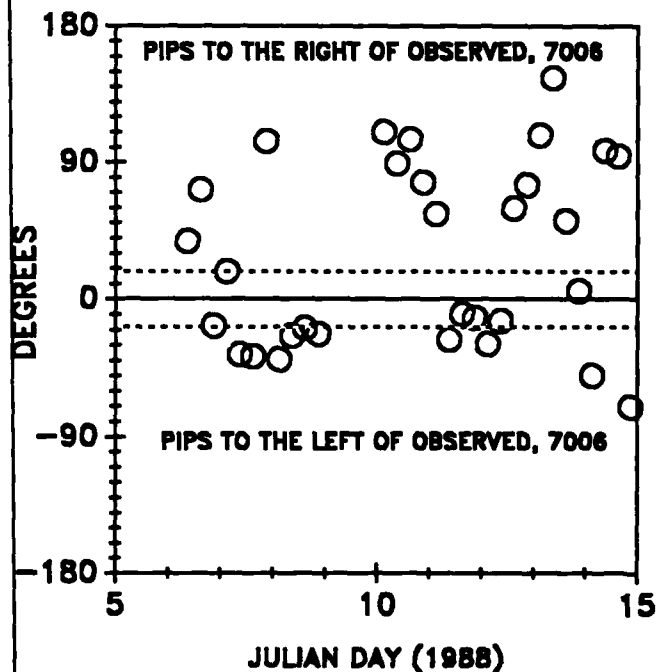


Fig. 15. Directional errors between the PIPS and 6 hr averaged ice motion at Buoy 7006 at the North Pole for January 1988. The dashed lines represent errors of  $\pm 18^\circ$  which are considered acceptable.

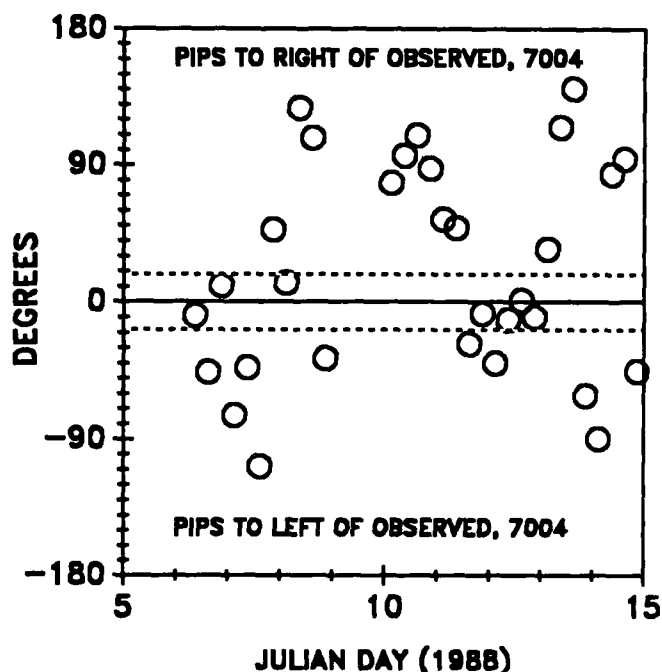


Fig. 16. Directional errors between the PIPS and 6 hr averaged ice motion at Buoy 7004 just south of the North Pole for January 1988. The dashed lines represent errors of  $\pm 18^\circ$  which are considered acceptable.

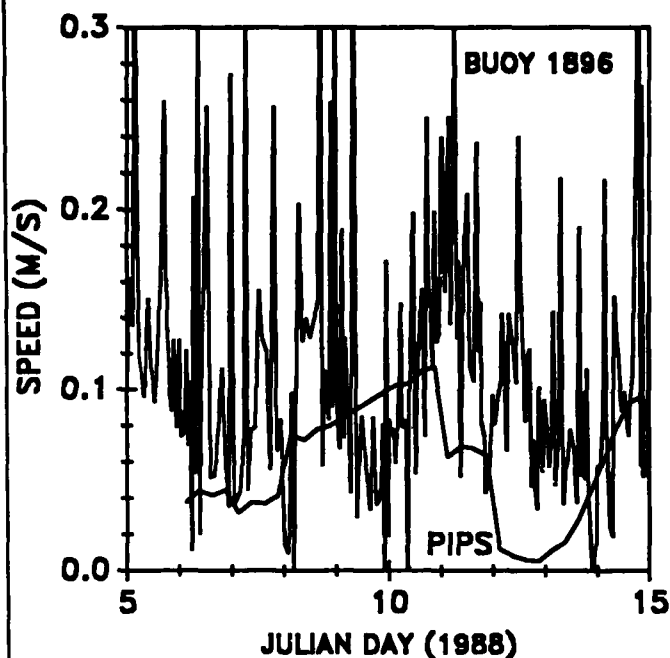


Fig. 17. A comparison of observed ice speeds at Buoy 1896 and PIPS ice speeds in the Chukchi Sea for January 1988.

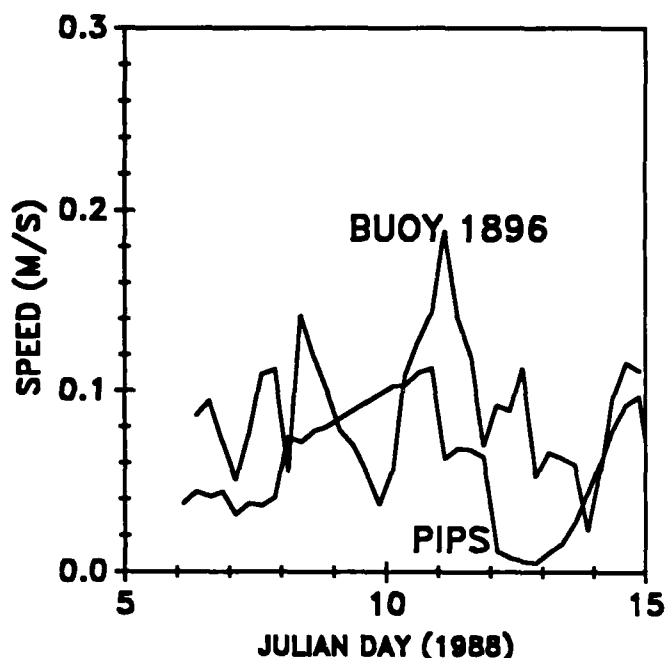


Fig. 18. A comparison of 6 hr averaged ice speeds at Buoy 1896 and PIPS ice speeds in the Chukchi Sea for January 1988.

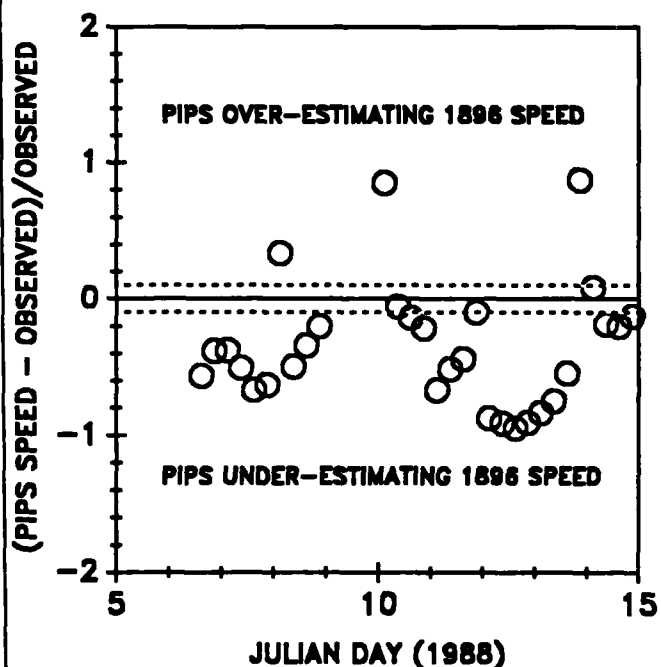


Fig. 19. Relative ice speed errors between the PIPS and 6 hr averaged ice speeds at Buoy 1896 in the Chukchi Sea for January 1988. The dashed lines represent errors of  $\pm 10\%$  which are considered acceptable.

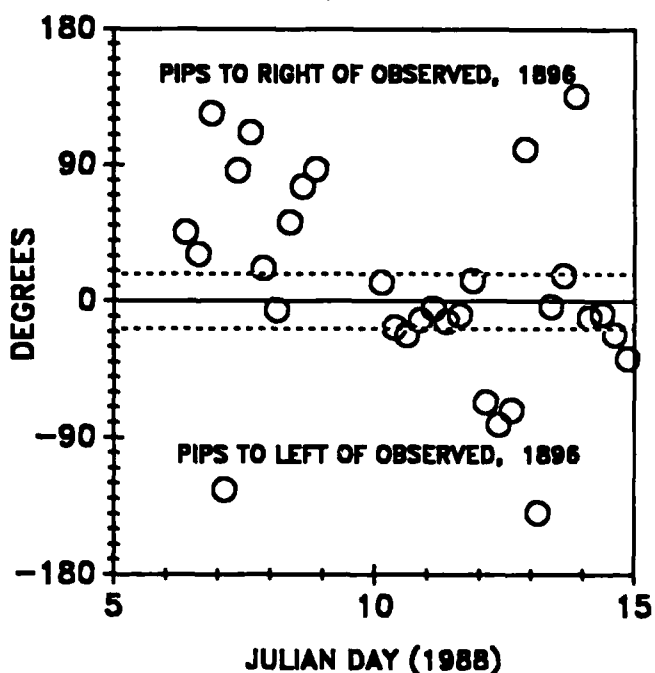


Fig. 20. Directional errors between the PIPS and 6 hr averaged ice motion at Buoy 1896 in the Chukchi Sea for January 1988. The dashed lines represent errors of  $\pm 18^\circ$  which are considered acceptable.

**SAIC**

### Some Comments

The variability of the buoy speed data is large compared to the model output. Much of this is likely the result of the model giving average speed variations over a 16000+ km<sup>2</sup> region. Thus, in our comparisons we should only be concerned with the model velocities following the trend of the observed velocities. However, we must also address the phase error between observed and modeled ice speed extremes.

The comparisons in the previous section were made to determine any distinct biases in the model's capability to predict ice motion. There does appear to be a trend for the model to over-estimate true ice speeds. A simplified force-balance argument would indicate that speed over-estimates (under-estimates) by the model should be accompanied by a direction of movement to the right (left) of observed motion. This is simply a result of the Coriolis effect being greater for larger ice speeds. Thus, one would have a greater deflection to the right in the northern hemisphere. To consider this, we constructed plots of directional differences versus relative speed errors. The North Pole data are shown in Fig. 21. In this case, the data tend to collect in the upper right quadrant, speed over-estimates associated with model motion to the right of observed motion. This would support our simple force-balance argument. This trend is not as strong in the data south of the pole (Fig. 22), but then again we are comparing a regional average velocity with a point measurement. Moreover, there are apparent phasing errors which could affect the expected relationship between directional bias versus over/under-estimations of the speed. However, this relationship is further supported by the November Chukchi Sea data (Fig. 23) but practically non-existent for the January Chukchi Sea region (Fig. 24). In the latter, we see a number of data points in the upper-left quadrant: under-estimating observed speeds while to the right of the observed motion vector.

In overcoming the tendency for the PIPS to over-estimate ice speeds, we do not recommend an adjustment of the wind stress on the ice. We recommend an adjustment of the estimated mass field of the ice pack. In those cases in which we had observations, we found that the PIPS underestimated ice thicknesses (up to a factor of 50%). This, of course, will lead directly to over-estimating ice speeds. In Section 3 of this report, we noted two critical problems with the PIPS methodology in determining ice thermal proper-

ties: the vertical resolution of the thermal wave in the ice and the thermal inertia of the ice. Both play a role in determining ice growth and decay. If these two problems are corrected in the PIPS, the model estimates of ice thicknesses should be more realistic, and this will lead to better estimates of ice velocity.

The phase differences between extremes of the observed and modeled data may at first seem like a rather minor point to address. However, the PIPS is an operational model for the Navy, and a 12 hr forecast error in the arctic might be critical. Thus, we should make some cursory comments on this phenomena. In all probability, the phase errors are a direct result of driving the PIPS by the Fleet Numerical Oceanography Center (FNOC) atmospheric model. This atmospheric model has a grid region of 77000+ km<sup>2</sup>, almost 5 times that of the PIPS. Thus, PIPS forcing (wind velocity, air temperature, radiation, etc.) must be determined by interpolating between the grid points of the atmospheric model. As a result, one can only estimate the locations of frontal systems as they traverse a region. The use of model winds along with the process of interpolation will almost always introduce some temporal phase shift between observed and modeled variables. And in some instances, particular variable extremes will be totally missed at given grid cells of the PIPS. This is an unavoidable problem. Some of the phase errors might be corrected by using an atmospheric model with a grid space more equal to that of the PIPS. That refinement should be determined based on the Navy's operational needs in the arctic.

In summary, we conclude the following:

- 1) The PIPS has a tendency to over-estimate ice speeds, and this is associated with directions that are to the right of the observed motion.
- 2) Better ice velocity predictions should be addressed by providing better ice thickness estimates through more precise model thermodynamics (see Section 3).
- 3) Errors in predicting ice velocity extremes and their times of occurrence are likely a result of the large grid size of the FNOC atmospheric model.
- 4) If greater precision is required in predicting the times of ice velocity extremes, the grid size of the atmospheric model should be halved (~150 km). This would also satisfy the requirements of predicting snow and cloud cover for input to PIPS.



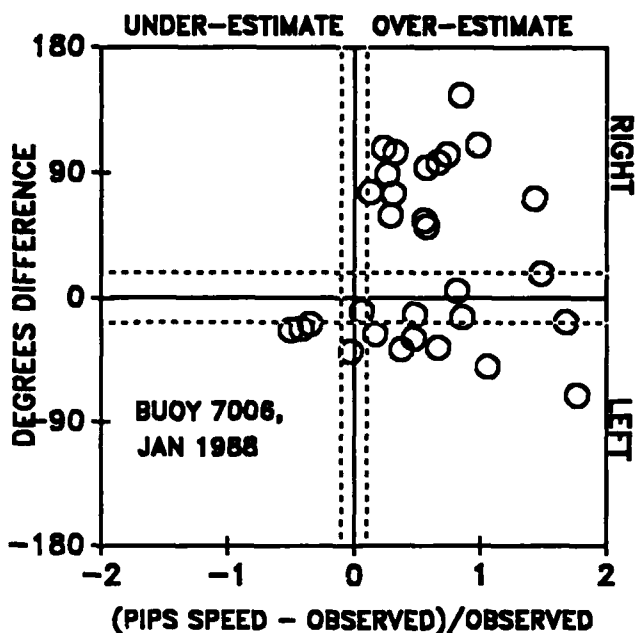


Fig. 21. A plot of the relationship between velocity magnitude and directional errors of the PIPS based on data from Buoy 7006 during January 1988. The dashed lines represent acceptable error limits of magnitude and direction.

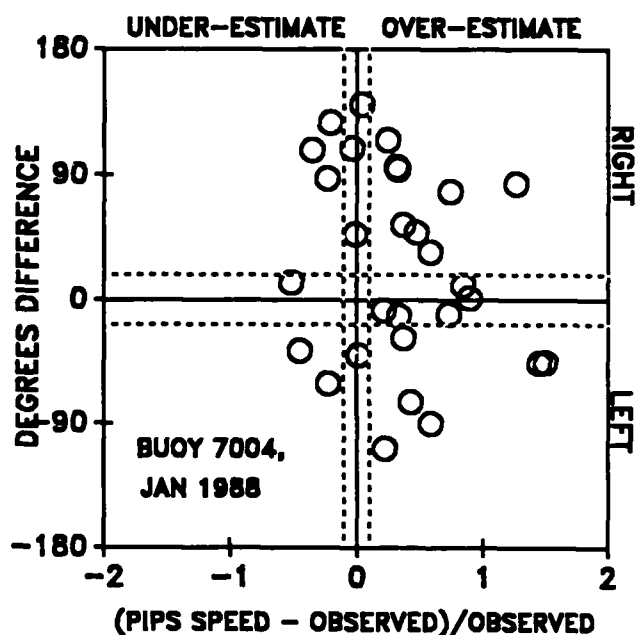


Fig. 22. A plot of the relationship between velocity magnitude and directional errors of the PIPS based on data from Buoy 7004 during January 1988. The dashed lines represent acceptable error limits of magnitude and direction.

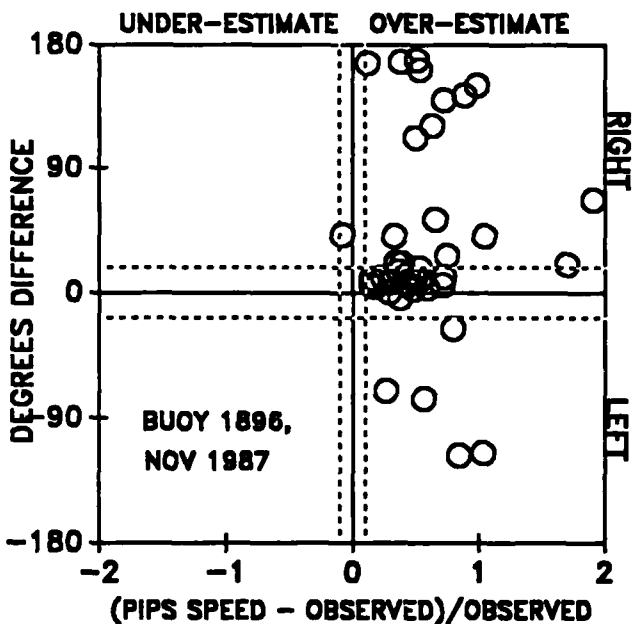


Fig. 23. A plot of the relationship between velocity magnitude and directional errors of the PIPS based on data from Buoy 1896 during November 1987. The dashed lines represent acceptable error limits of magnitude and direction.

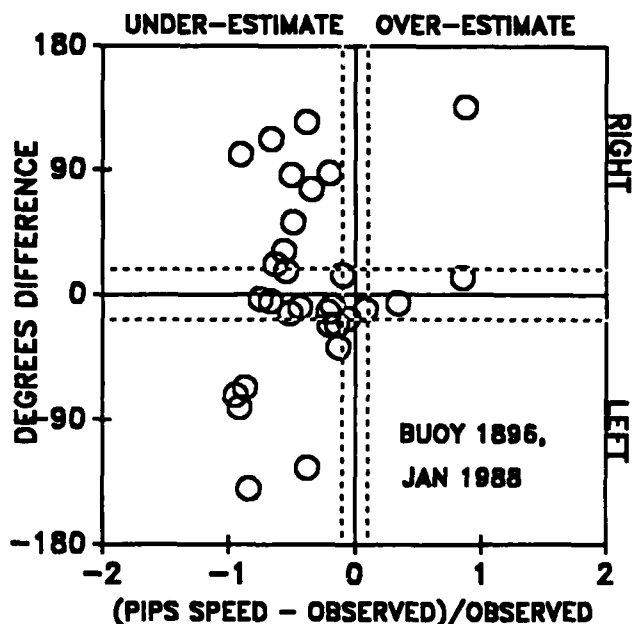


Fig. 24. A plot of the relationship between velocity magnitude and directional errors of the PIPS based on data from Buoy 1896 during January 1988. The dashed lines represent acceptable error limits of magnitude and direction.

**SAIC**

### ACKNOWLEDGMENTS

This work was supported by the United States Navy, ASW Oceanography Program, at the Naval Ocean Research and Development Activity, NSTL, Mississippi.

### REFERENCES

- Colony, R., and A. S. Thorndike, 1984: An estimate of the mean field of arctic sea ice motion. *J. Geophys. Res.*, 89 (C6), 10623-10629.
- Cushman-Roisin, B., Heil, W. H., and Nof, D., 1985: Oscillations and rotations of elliptical warm-core rings. *J. Geophys. Res.*, 90, 11756-11764.
- Hibler, W. D., III, 1979: A dynamic thermodynamic sea ice model. *J. Phys. Oceanogr.*, 9, 815-846.
- Hibler, W. D., III, and W. B. Tucker, III, 1979: Some results from a linear-viscous model of the arctic-ice cover. *J. Glaciology*, 22 (87), 293-304.
- Tucker, W. B., III, and W. D. Hibler, III, 1987: An evaluation of the Polar Ice Prediction System. U.S. Army Cold Regions Research and Eng. Lab., Hanover, N.H., 94 pp.
- Kirwan, A. D., and M. S. Chang, 1979: Effect of sampling rate and random position error on analysis of drifter data. *J. Phys. Oceanogr.*, 9, 382-387.
- Lewis, J. K., and W. W. Denner, 1988: Higher Frequency Ambient Noise in the Arctic Ocean. A report to the Off. of Naval Res., Sci. Appl. Int'l. Corp. Tech. Rep. SAIC-87/1868. 25 pp.
- Lewis, J. K., M. R. Giuffrida and W. W. Denner, 1988: Sea Ice Kinematics: Space and Time Scales. A report to the Naval Research and Development Activity, Sci. Appl. Int'l. Corp. Tech. Rep. SAIC-87/1870. 35 pp.
- Manabe, S., K. Bryan, and M. J. Spelman, 1979: A global ocean-atmosphere climate model with seasonal variation for future studies of climate sensitivity. *Dyn. Atmos. Ocean.*, 3, 393-426.
- McPhee, M. G., 1978: The free drift velocity field across the AIDJEX manned camp array. *AIDJEX Bull.* 38, Univ. of Wash., 158-163.
- Parkinson, C. L., and W. M. Washington, 1979: A large-scale numerical model of sea ice. *J. Geophys. Res.*, 84, 311-337.
- Popelar, J., and J. Kouba, 1983: Satellite Doppler determination of differential sea ice motion in the vicinity of the North Pole. *Marine Geodesy*, 7, 171-198.
- Preller, R. H., 1985: The NORDA/FNOC Polar Ice Prediction System (PIPS) - Arctic: A technical description. NORDA Rep. 108, NSTL, Miss., 60 pp.
- Semtner, A. J., 1976: A model for the thermodynamic growth of sea ice in numerical investigations of climate. *J. Phys. Oceanogr.*, 6, 379-389.
- Thorndike, A. S., 1986: Kinematics of sea ice. In *The Geophysics of Sea Ice* (N. Untersteiner, ed.). Plenum Press, New York, 489-549.

The logo for SAIC (Science Applications, Inc.) is located in the bottom right corner of the page. It consists of the letters "SAIC" in a bold, italicized, sans-serif font. The letters are white with a black outline, and they are set against a dark, textured background that resembles a stylized wave or a dense pattern of small dots.